Characterization of Extra-Framework Cation Positions in Zeolites NaX and NaY with Very Fast ^{23}Na MAS and Multiple Quantum MAS NMR Spectroscopy

Kwang Hun Lim and Clare P. Grey*

Contribution from the Department of Chemistry, SUNY Stony Brook, Stony Brook, New York 11794-3400

Received April 12, 2000. Revised Manuscript Received June 28, 2000

Abstract: ^{23}Na MAS and two-dimensional multiple quantum MAS (MQMAS) NMR techniques have been used to identify the sodium cations in zeolites NaX and NaY, and to investigate changes in the distribution of the sodium cations on adsorption of hydrofluorocarbon-134 (HFC-134, CF_2HCF_2H), -134a (CF_3CFH_2), -125 (CF_3CF_2H), and -143 (CF_2HCFH_2). ^{23}Na NMR parameters determined from the MQMAS NMR spectra (acquired with high ^{23}Na radio frequency power) were used for quantitative analysis of the ^{23}Na MAS NMR spectra, obtained at very fast spinning frequencies (21 kHz). At room temperature, four (I, II, I′, and hydrated sodium cations) and five (I, two III′, II, and I′) sodium sites were identified in NaY and NaX, respectively. Cation occupancies for the different sites were also obtained following sorption of HFC-134, again from the MQMAS and fast MAS spectra. For zeolite NaY, the distribution of the extra-framework cations changed significantly, the SI′ cations migrating into the SI site and into the supercages (resulting in occupancy of the SIII′ sites), presumably to optimize cation−HFC interactions. No significant change in the SI′ cation population was detected following sorption of HFC-134 on zeolite NaX. However, two SI sites, due to different local environments for the cations, within the hexagonal prisms, were observed. Variable-temperature ^{23}Na MAS and 2D MQMAS NMR experiments were performed on bare NaY, to probe rearrangement of the sodium cations above room temperature. The SI resonance was observed to decrease in intensity above 150 °C, and a new resonance was seen. A two-dimensional ^{23}Na-exchange NMR experiment, performed at 250 °C, revealed considerable cation mobility involving the supercage cation sites.

Introduction

Extra-framework cations play an important role in determining the adsorption, separation, and catalytic properties of zeolites. The positive charge of the extra-framework cations produces electric fields within the zeolite pores, which can strongly influence absorptive behavior and catalytic activity.[1,2] Since the distribution of the cations controls the electric fields, the characterization of the cation sites is a prerequisite for understanding of the physical properties of zeolites. The locations of the extra-framework cations in bare, dehydrated faujasite zeolites such as NaX and Y have been determined by X-ray and neutron diffraction (Figure 1).[3−5] Sites I and I′ are located in the hexagonal prism and the sodalite cage, respectively, while the site II and III positions are in the supercage. In dehydrated zeolite NaY, the sodium cations are mainly located on the site I, I′, and II positions.[2,4] Sodium cations are also found in several sites close to the site III position, in dehydrated NaX, which has a higher sodium content than NaY. These cations may not be regarded as fixed species and recent work has, for example, shown that both the occupancy and positions of the extra-framework cations often change during the dehydration process or on adsorption of gas molecules.[6−8] Thus a fuller understanding of the role that the extra-framework cations play in controlling sorption and catalytic properties requires that careful structural studies are performed under as real as possible conditions, which closely mimic those of the sorption or catalytic environments (for example, under realistic gas partial pressures and temperatures).

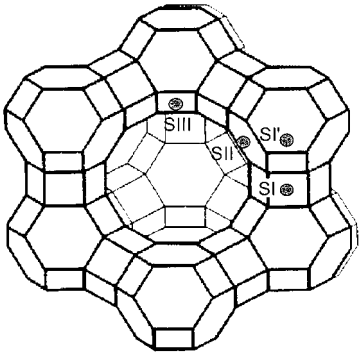

Figure 1. A representation of the framework of a faujasite-type zeolite and possible locations of the extra-framework cations.

We have been studying the binding of hydrofluorocarbons (HFCs) such as the refrigerant HFC-134a (CF_3CFH_2) and its symmetric isomer HFC-134 (CF_2HCF_2H) to rationalize the differences in binding of these different HFCs on basic zeolites, to provide a fundamental basis for the proposals to use these

(1) Breck, D. *Zeolite Molecular Sieves*; John Wiley & Sons: New York, 1974.
(2) Mortier, W. J. *Compilation of Extraframework Sites in Zeolites*; Butterworth-Heineman: London, 1982.
(3) Mortier, W. J.; Bossche, E. V. d.; Uytterhoeven, J. B. *Zeolites* **1984**, *4*, 41.
(4) Fitch, A. N.; Jobic, H.; Renouprez, A. *J. Phys. Chem.* **1986**, *90*, 1311.
(5) Olson, D. H. *Zeolites* **1995**, *15*, 439.
(6) Stahl, K.; Artioli, G.; Hanson, J. C. *Phys. Chem. Minerals* **1996**, *23*, 328.
(7) Norby, P.; Poshni, F. I.; Gualtieri, A. F.; Hanson, J. C.; Grey, C. P. *J. Phys. Chem. B* **1997**, *102*, 839.
(8) Grey, C. P.; Poshni, F. I.; Gualtieri, A. F.; Norby, P.; Hanson, J. C.; Corbin, D. R. *J. Am. Chem. Soc.* **1997**, *119*, 1981.

10.1021/ja001281d CCC: $19.00
Published on Web 09/21/2000

basic zeolites as a method for separating different HFC and hydrochlorofluorocarbon mixtures produced in the synthesis of the HFCs.[9] In a joint ^{23}Na NMR and XRD study, we showed that sorption of HFC-134 on zeolite NaY results in a long-range migration of SI′ cations from the sodalite cages and into the supercages, where they can coordinate to the HFC molecules. The ^{23}Na NMR, although obtained at a relatively slow spinning speed of 10 kHz, showed that the SI′ cations were affected by gas binding, the gas binding resulting in a reduction of the quadrupole coupling constant (QCC) of the cations originally in the SI′ positions. It was not possible to determine exactly where in the supercages the cations migrated to, but SI′ migration was proposed to result in occupancy of SIII-type sites, since the SII positions were already full in the bare material. In some of the systems studied, particularly at slow spinning speeds and at very low gas loading levels, it was very difficult to quantify the numbers of the few remaining SI′ cations that were not affected by gas sorption, since their resonances are obscured by the spinning sidebands of the resonances of the SII cations. The XRD diffraction data were extremely useful as a complementary tool to pin down cation migration, and were essential in providing a structural model for how the HFC-134 molecule is bound to the Na^+ cations and the framework.

In many systems, it is not practical (or indeed possible) to solve the structure of the gas-loaded sample, with powder X-ray or neutron diffraction data, to determine exactly where the cations and gas molecules are located following gas sorption. Thus, in subsequent experiments, we have used ^{19}F→^{23}Na cross-polarization (CP) experiments to probe the modes of binding in a whole series of asymmetric HFCs (e.g., HFC-134a, -125 CF_3CF_2H, and -143 CF_2HCFH_2).[10,11] These CP studies showed preferential binding of the CFH_2 group to the sodium cation, the weakest interaction being observed for the CF_3 group. This was ascribed to a combination of hydrogen bonding to the oxygen atoms of the zeolite framework and the greater negative charge of fluorine atoms in the hydrogen-containing end groups. Very similar Na^+−HFC interactions were observed for NaX and NaY, despite the lower cation content of the former zeolite.[10,12] Cheetham et al. have investigated HFC and hydrochlorocarbon binding in similar zeolites by using a combination of molecular modeling and inelastic neutron scattering approaches; these studies also highlighted the importance of the hydrogen-bonding interactions.[13−15]

Both double resonance NMR and X-ray diffraction methods (as applied to loaded systems) typically yield better structural data when the experiments are performed at low temperatures, where the molecules are more ordered (XRD) and the translational motion is frozen out (XRD and NMR). Thus experiments still need to be performed to bridge the gap between the low-temperature structural determinations and the structure and cation positions at more elevated temperatures. Thus, one purpose of this paper is to examine NMR methods for determining cation positions at room temperatures, and to determine the effect of gas binding on the cation positions (of NaY and NaX) at these temperatures.

Solid-state ^{23}Na MAS NMR is very sensitive to the sodium local environment, and thus has been widely used to characterize the sodium cations in zeolites NaX and NaY.[8,16,17] However, the interpretation of the ^{23}Na MAS NMR spectra is not always straightforward due to the overlap of the resonances, as a result of the second-order quadrupolar interaction. Double rotation (DOR) NMR[18,19] has been widely employed to obtain high-resolution ^{23}Na NMR spectra of zeolites, by removing the second-order quadrupolar interaction.[17,20−22] Two types of I′ sites, with slightly different local environments, were observed in an X-ray diffraction (XRD) study of a single crystal of NaX (Si/Al: 1.18).[5] A six-membered ring in the faujasite structure is made up of, at most, three aluminum atoms per ring. If the six-membered rings that contain zero or only one aluminum atom (which represent the least probable arrangements in NaX zeolites) are ignored, then ∼24 and 8 six-membered rings per unit cell have three and two aluminum atoms per ring, respectively, for a Si/Al ratio of 1.18 ($Na_{88}Si_{104}Al_{88}O_{384}$). Site I′ sodium cations can be coordinated to both of these types of six-membered rings.[5] Electric field gradient (EFG) calculations have shown that the QCC for the site I′ sodium cations coordinated to the six-membered rings containing three aluminum atoms (5.0 MHz) is larger than that for the site I′ cations coordinated to the rings with only two aluminum atoms (3.6 MHz).[17] The ^{23}Na DOR NMR spectrum of NaX (Si/Al: 1.23) could be well reproduced by a computer simulation, which used ^{23}Na NMR parameters for six different sodium cations (site I, II, and III′ (two sites), and the two types of site I′ cations).[17] However, the central resonances overlapped with some of the spinning sidebands in the ^{23}Na DOR NMR spectra, rendering the assignment of the sodium cation resonances ambiguous. The recently developed two-dimensional multiple quantum MAS (MQMAS)[23,24] technique has also been used to investigate the locations of the sodium cations in NaY (Si/Al: 2.4 and 2.6), NaEMT (3.7), NaMOR (7.1), and NaZSM-5 (18.0).[25,26] ^{23}Na NMR parameters could be determined more accurately than from a single pulse spectrum alone, by comparing the parameters obtained from the position of the NMR resonances in the isotropic dimension of the 2D MQMAS NMR spectra, with those obtained from the 1-dimensional spectra. The QCC value for the sodium cations located at the site I position in NaY and NaEMT was found to be 1.2 MHz, which was much larger than expected. It was proposed that the site I position is displaced from the center of the hexagonal prism, resulting in the large QCC value.[27] The sodium cations at the site I′ in zeolite NaY were not observed in the previous MQMAS NMR spectra, and the MQMAS method has not been applied to study zeolite NaX.

A different interpretation of the effect of gas binding on the SI′ QCC has been recently presented by Bosch et al.[28] A large

(9) Corbin, D. R.; Mahler, B. A. World Patent 94/02440 (1994). Yoneda, S.; Takei, R.; Yanase, K. Japanese Patent 91/97969, 1994. Edwards, D. W. G. B. Patent 91-5421, 1994; European Patent 503796, 1994. Ono, H.; Tsuji, K.; Nakayama, H. Japanese Patent JP 89-207497, 1992.
(10) Lim, K. H.; Grey, C. P. In preparation.
(11) Lim, K. H.; Grey, C. P. *Chem. Commun.* **1998**, *20*, 2257.
(12) Lim, K. H. Ph.D. Thesis, SUNY Stony Brook, 2000.
(13) Mellot, C. F.; Cheetham, A. K.; Harms, S.; Savitz, S.; Gorte, R. J.; Myers, A. L. *J. Am. Chem. Soc.* **1998**, *120*, 5788.
(14) Mellot, C. F.; Cheetham, A. K.; Harms, S.; Savitz, S.; Gorte, R. J.; Myers, A. L. *Langmuir* **1998**, *14*, 6728.
(15) Mellot, C. F.; Cheetham, A. K. *J. Phys. Chem. B* **1999**, *103*, 3864.
(16) Engelhardt, G.; Hunger, M.; Koller, H.; Weitkamp, J. *Stud. Surf. Sci. Catal.* **1994**, *84*, 725.
(17) Feuerstein, M.; Hunger, M.; Engelhardt, G.; Amoureux, J. P. *Solid State NMR* **1996**, *7*, 95.
(18) Wu, Y.; Sun, B. Q.; Pines, A.; Samoson, A.; Lippmaa, E. *J. Magn. Reson.* **1990**, *89*, 297.
(19) Samoson, A.; Lippmaa, E.; Pines, A. *Mol. Phys.* **1988**, *65*, 1013.
(20) Jelinek, R.; Ozkar, S.; Pastore, H. O.; Malaek, A.; Ozin, G. A. *J. Am. Chem. Soc.* **1993**, *115*, 563.
(21) Jelinek, R.; Malaek, A.; Ozin, G. A. *J. Phys. Chem.* **1995**, *99*, 9236.
(22) Koller, H.; Overweg, A. R.; Santen, R. A. V.; Haan, J. W. D. *J. Phys. Chem.* **1997**, *101*, 1754.
(23) Frydman, L.; Harwood, J. S. *J. Am. Chem. Soc.* **1995**, *117*, 5367.
(24) Medek, A.; Harwood, J. S.; Frydman, L. *J. Am. Chem. Soc.* **1995**, *117*, 12779.
(25) Hu, K. N.; Hwang, L. P. *Solid State NMR* **1998**, *12*, 211.
(26) Hunger, M.; Sarv, P.; Samoson, A. *Solid State NMR* **1997**, *9*, 115.
(27) Engelhardt, G. *Microporous Mater.* **1997**, *12*, 369.
(28) Bosch, E.; Huber, S.; Weitkamp, J.; Knozinger, H. *Phys. Chem. Chem. Phys.* **1999**, *1*, 579.

reduction in the QCC of the SI′ cation was also observed in their ^{23}Na MAS NMR study of $CHCl_3$ binding on NaY, which was ascribed to a change in the charge distribution induced by the hydrogen bonding of the gas to the negatively charged oxygen atoms of the zeolites framework, and was not considered to be an indication of any changes in cation occupancies. Thus, in the present study, the results of the ^{23}Na MAS and 2D MQMAS NMR studies of zeolites NaX (Si/Al: 1.25) and NaY (2.6) are presented. A high ^{23}Na radio frequency field strength (200 kHz) and very fast MAS (21 kHz) are used for the MQMAS NMR experiments, to identify the very large QCC sites (such as the site II and I′ cations) in NaX and NaY. Quantitative analysis of the very fast ^{23}Na MAS NMR spectra with the NMR parameters obtained with the MQMAS NMR experiments are performed. With these results as a foundation, the changes in the occupancy, and the QCCs of the extra-framework cations, following adsorption of HFC-134 and -134a are then investigated and the proposal of Bosch et al.[28] is carefully tested.

In the last section of the paper variable-temperature ^{23}Na MAS, two-dimensional ^{23}Na magnetization exchange,[29] and another MQMAS technique, rotationally induced adiabatic coherence transfer (RIACT) MQMAS,[30] which has been shown to be less sensitive to the quadrupole interaction, are all used to probe rearrangement and motion of the extra-framework cations above room temperature, in dehydrated NaY.

Experimental Section

Sample Preparation. Zeolites NaX and NaY were dehydrated on a vacuum line by slowly ramping the temperature to 400 °C over a period of 48 h. HFC-loaded zeolite samples were prepared by exposing controlled amounts of the HFC molecules to the dehydrated zeolites at room temperature. The loading level of the sample was determined by observing the pressure drop of the HFC gas in a carefully calibrated vacuum line. Fully loaded samples were prepared by exposing the gas to the zeolite until no further drop in pressure was detected. Samples are labeled *x*HFC/NaY, where *x* indicates the number of HFC molecules per supercage (s.c.). A fully loaded sample corresponds to a loading level of approximately 6−7 molecules per s.c. All samples were then packed in ZrO_2 rotors in a glovebox under dry N_2. The Si/Al ratios of NaX (1.25) and NaY (2.6) were determined from their ^{29}Si MAS NMR spectra.

NMR Measurements. All NMR spectra were acquired with Chemagnetics probes, on a CMX-360 spectrometer at 95.2 MHz for ^{23}Na. The ^{23}Na NMR spectra acquired with very fast MAS (∼21 kHz) were obtained with a 3.2 mm probe, while all other NMR spectra were obtained using a 5 mm probe with a spinning speed of 10 kHz. Small flip angles (∼15°) were used for quantitative analysis of the ^{23}Na MAS NMR spectra. The ^{23}Na MQMAS NMR spectra were obtained by using either the *z*-filtered three-pulse sequence[31] or the RIACT method.[30] A ^{23}Na radio frequency field strength of 200 kHz and a spinning speed of 21 kHz were used for the *z*-filtered three-pulse MQMAS NMR experiments, while a ^{23}Na radio frequency field strength of 100 kHz and a spinning speed of 10 kHz were used for the RIACT MQMAS NMR experiments. The hypercomplex method was employed to obtain pure-absorption 2D NMR spectra.[32] The ^{23}Na chemical shifts were referenced to 1 M NaCl solution (−7 ppm relative to solid NaCl) at 0.0 ppm. The real sample temperature was determined by calibrating the Chemagnetics variable-temperature (VT) equipment with the shift of $Pb(NO_3)_2$[33] at various measured temperatures, at the same drive and bearing pressures as used in the ^{23}Na NMR experiments.

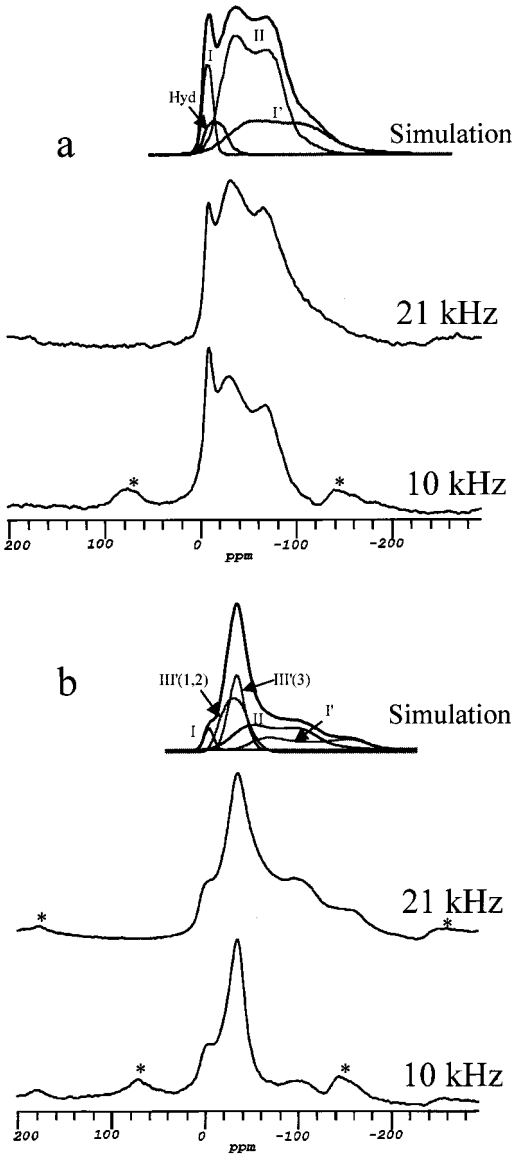

Figure 2. The ^{23}Na MAS NMR spectra of dehydrated (a) NaY and (b) NaX acquired at two spinning speeds (10 and 21 kHz). An asterisk indicates spinning sidebands. Simulations of the isotropic resonance of the central transitions of NaY and NaX, at a spinning speed of 21 kHz, are shown above the experimental spectra. The individual contributions to the total sum from the different cation sites are shown, for each simulation. Values for Ω, obtained from the MQMAS data, were used as constraints in the simulations of the spectra (see text and Figure 3).

Results

Bare NaX and NaY. Figure 2 shows the strong dependence of the ^{23}Na MAS NMR spectra of NaY (a) and NaX (b) on the MAS spinning speed. For NaY, the relative intensity of the broader resonances, spreading from approximately −25 to −140 ppm, increases at the higher spinning speed of 21 kHz. The broad resonance in NaX that gives rise to the shoulders at approximately −160 ppm is clearly observed at the spinning speed of 21 kHz, but is not detected at 10 kHz. These spectra demonstrate that very fast MAS is required to investigate a large QCC system at the moderate magnetic field strength (8.45 T) used in this study. The very fast ^{23}Na MAS NMR spectra of NaX and Y are similar to previously reported spectra measured at a higher magnetic field strength of 11.7 T.[16,17] Based on these

(29) Jeener, J.; Meier, B. H.; Bachmann, P.; Ernst, R. R. *J. Chem. Phys.* **1973**, *71*, 4546.
(30) Wu, G.; Rovnyank, D.; Griffin, R. G. *J. Am. Chem. Soc.* **1996**, *118*, 9326.
(31) Amoureux, J. P.; Fernandez, C.; Steuernagel, S. *J. Magn. Reson.* **1996**, *A123*, 116.
(32) Massiot, D.; Touzo, B.; Trumeau, D.; Coutures, J. P.; Virlet, J.; Florian, P.; Grandinetti, P. J. *Solid State NMR* **1996**, *6*, 73.
(33) Bielecki, A.; Burum, D. P. *J. Magn. Reson.* **1995**, *116*, 215.

previous studies, the narrow resonance at −6 ppm in the NaY spectrum (Figure 2a) is assigned to the site I cations, and the broad powder pattern caused by the second-order quadrupolar interaction is assigned to the two overlapping resonances from the site II and I′ cations. EFG calculations have shown that the QCC for the site II cations is smaller than that for the site I′ cations.[17] In addition, the number of site II cations is larger than the number of site I′ cations.[4] Thus, the two singularities centered at −30 and −70 ppm have been ascribed to the same second-order powder pattern arising from the site II cations.[16,17] The broad resonance ranging from −100 to −160 ppm is too broad and intense to be assigned to the foot of the powder pattern containing the two singularities centered at −30 and −70 ppm. Moreover, the intensity of this resonance increases significantly at higher spinning speeds, suggesting that it is primarily due to part of a resonance from a larger QCC site. Therefore, the broad feature is assigned to the site I′ cations. In the NaX spectrum (Figure 2b), the resonance at 1 ppm is assigned to the site I cations, and the resonance at approximately −33 ppm is assigned to the site III′ cations. The broad shoulders at −100 and −160 ppm can be assigned to the singularities in the powder pattern for the site II and I′ cations, respectively, since the QCC for the site I′ cations is known to be large, in comparison to that for the site II cations.[17]

Figure 3 shows the 2D MQMAS NMR spectra of dehydrated NaY (a) and NaX (b). Signals from the site I and II cations are clearly detected in the spectrum of NaY, as in the previous reported spectra.[25,26] However, sodium cations at the site I′ position, which were not detected in the previous study, are also observed at a slightly larger value of F1. The small resonance −20 ppm in the F2 dimension is attributed to hydrated sodium cations. The 2D MQMAS NMR spectrum of NaX shown in Figure 3b consists of five sodium sites. Two different site III sodium cations, which were not clearly resolved due to the overlapping resonances in the ^{23}Na MAS NMR spectrum, are split into two sites. Signals from the site II and I′ cations are also observed in the MQMAS NMR spectrum. However, the relative intensities of the site II and I′ cations are significantly reduced, in comparison to those in the 1D MAS spectrum (Figure 2a). This is due to the fact that the efficiency of the MQMAS experiment drastically decreases for large QCC sites (such as the site II and I′ cations). The NMR parameters can be extracted by calculating the position of the resonance in the isotropic dimension of the 2D MQMAS NMR spectrum, Ω, which is given, for $S = {}^3/_2$ nucleus, by:[34]

$$\Omega = \frac{34}{9}\delta_{iso} + \frac{[2\omega_Q{}^2(3+\eta^2)] \times 10^6}{27\omega_0{}^2} - \frac{34}{9}\delta_{offset} \quad (1)$$

where δ_{iso} and ω_0 are the isotropic shift and Larmor frequency, respectively, and ω_Q is the first-order quadrupolar frequency, which is related to the quadrupole coupling constant (QCC or $e^2qQ/\hbar$) by:

$$\omega_Q = \frac{3e^2qQ}{2\hbar} \quad (2)$$

The signals from the large QCC sites (II and I′) are significantly broadened in the isotropic dimension of the 2D MQMAS NMR spectra, which results in a considerable amount of uncertainty for the NMR parameters extracted from the MQMAS NMR spectra for the large QCC sites. The MAS NMR spectra were, therefore, simulated to test the reliability of the

(34) Hanaya, M.; Harris, R. K. *J. Phys. Chem.* **1997**, *A101*, 6903.

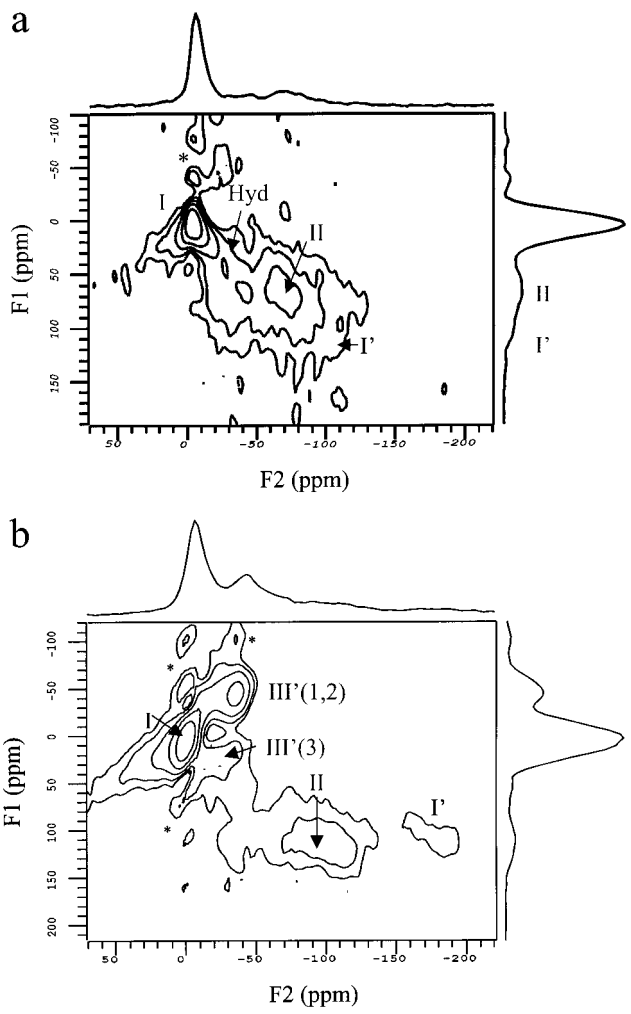

Figure 3. Two-dimensional ^{23}Na triple quantum MAS NMR spectra of (a) NaY and (b) NaX, after shearing. t_1 increments of 7.8 and 12.8 μs were used for NaX and NaY, respectively. 512 (t_2) × 23 (t_1) and 512 (t_2) × 29 (t_1) hypercomplex data points, and 7200 and 6000 FIDs per t_1 increment, were acquired for NaX and NaY, respectively, and zero-filled to 512 (t_2) × 128 (t_1). Projections on the isotropic (F1) and anisotropic (F2) dimensions are shown. An asterisk denotes the artifacts originating from insufficient t_1 data points. ^{23}Na radio frequency field strength = 200 kHz; spinning speed = 21 kHz.

NMR parameters obtained with the MQMAS method and to obtain accurate site populations. Good fits to the experimental spectra were obtained for both NaY and NaX (Figure 2). The discontinuity at ca. −110 ppm due to the SI′ cations is less pronounced in the experimental spectrum than in our simulated spectrum indicating that there is a small distribution of SI′ environments. This also explains why the SI′ positions are not so clearly resolved in the MQMAS spectrum. The ^{23}Na NMR parameters obtained from the 2D MQMAS and the simulation of the MAS NMR spectra (Table 1) are in good agreement with the previous reported values,[17] except for the SII and I′ cations in NaX where the QCCs are slightly larger than those obtained previously. A significantly smaller QCC is obtained for one SIII′ site, and on that basis we assign this site to the more symmetrical SIII′ site (SIII′(3) in ref 17 and Na5 in ref 5). Thus the other distorted SIII′ site is labeled SIII′(1,2), using the notation of ref 18. The relative populations of the sodium cations were also extracted from the simulation of the MAS NMR spectrum. However, the relative intensities in the ^{23}Na MAS NMR spectra need to be corrected since the relative intensity is strongly dependent on the spinning speed (ω_r), the Larmor frequency

Table 1. ^{23}Na NMR Parameters for Dehydrated NaY and NaX Obtained by 2D MQMAS NMR and by Simulating the ^{23}Na MAS NMR Spectra[a]

					Na/uc	
	Ω/ppm (calcd value)	δ_{iso}/ppm (lit.)	QCC/MHz (lit.)	η (lit.)	this work	X-ray[8,5]
Na						
SI	3 ± 1 (3.2)	−1.5	1.2 ± 0.1	0 + 0.1 (0)	3	4.3
SI′	96 ± 5 (96)	−12 (3.5)	4.8 ± 0.15 (4.8)	0 + 0.1 (0.2)	17	18.9
SII	64 ± 5 (64)	−8 (−5)	3.9 ± 0.15 (4.0)	0 + 0.1 (0.2)	30	32
Hydr.	36 ± 2 (36)	1	2.3 ± 0.1	0 + 0.1 (0)	3	
NaX						
SI	1.8 ± 1 (1.8)	−2.7	1.4 ± 0.1	0 + 0.1	2	2.9/—[b]
SI′	109 ± 5 (109)	−20 (−13)	5.4 ± 0.15 (5.0)	0 + 0.1 (0)	28	21/25[b]
SI′	− (−)	− (−21)	− (3.6)	− (0)	−	8/8[b]
SII	106 ± 5 (106)	−10 (−11)	4.9 ± 0.15 (4.5)	0 + 0 (0.1)	32	31/30[b]
SIII′(1,2)	19 ± 1 (19)	−11 (−4)	3.0 ± 0.1 (3.0)	0.5 ± 0.1 (0.5)	13	19/13[b]
SIII′(3)	−46 ± 1 (−46)	−21 (−24)	2.1 ± 0.1 (1.9)	0.9 ± 0.1 (0.9)	10	11/10[b]

[a] The calculated values for Ω, obtained by inputting the values of the QCC, η, and δ_{Iso} used in the simulations of the MAS spectra into eq 1, are compared with the values of Ω extracted from the MQMAS spectra. The values for the QCC, η, and δ_{Iso} are compared with literature values given in ref 17; cation occupancies (per unit cell (uc)) are compared with those obtained from X-ray studies of NaY[8] and NaX (Si/Al = 1.18)[5] and with occupancies obtained by NMR for NaX (Si/Al = 1.23)[17] [b] NMR values.

(ω_0), and the first-order quadrupolar frequency (ω_Q).[35] The relative intensity was, therefore, corrected from the intensity vs $\omega_Q^2/(\omega_r\omega_0)$ curve calculated by Massiot et al.,[35] and the results for NaY and NaX are shown in Table 1. The results are quite consistent with the X-ray diffraction results of our sample (NaY) and the previous report for NaX (Si/Al:1.23).[8,17] Importantly, the joint MAS and MQMAS NMR study allows for an accurate determination of the number of SI′ cations.

HFC-134/NaY. Figure 4 shows ^{23}Na MAS NMR spectra, as a function of HFC-134 loading level, obtained at a spinning speed of 21 kHz. As the loading level is increased, the broad resonances from the site II and I′ cations narrow considerably due to a reduction of the QCCs of the nuclei at these sites, and a resonance centered at −33 ppm grows in intensity. This was observed in our previous NMR study performed at a spinning speed of 10 kHz.[8] However, changes in line widths and intensities of the NMR resonances of the site I′ cations (∼ −100 ppm) are now clearly observed at fast MAS.

Figure 5 shows the ^{23}Na MQMAS NMR spectra of (a) 2HFC-134/NaY and (b) fully loaded HFC-134/NaY. Three sodium sites are observed in both spectra, the positions of the signals changing according to the loading level. The signals from the site I cations remain in similar positions, while the signals from the site II cations and the new resonance shift to lower frequencies in the isotropic dimension (F1) with increased gas loading (compare Figure 3a and 5). ^{23}Na NMR parameters for the two samples were obtained by calculating the positions of the resonances in the F1 dimension using eq 1, and are shown in Table 2. The experimental MAS NMR spectra were well reproduced by the computer simulations with these NMR parameters, as is shown in Figure 6.

A comparison of the results shown in Tables 1 and 2 shows that the QCCs of the sodium cations originally in the site II and I′ cations are significantly reduced on adsorption of HFC-134 molecules (see Table 1), particularly at high loading levels; no evidence for any site with a QCC of the same order of magnitude of the original SI′ position is observed, even at the relatively low loading level of 2 molecules/s.c. The reduction of the QCC of the SII position depends on the loading level: at low loading levels no significant change is observed, while at higher loading levels the change is significant. A reduction in the occupancy of the SII site is also observed at higher loading levels, in agreement with the XRD results.[8] An increase in the SI population is seen with increased loading level, which is consistent with a decrease in the population of the site I′ cations, since the site I and I′ positions cannot be occupied simultaneously. There is a reasonable agreement with cation occupancies obtained by NMR and diffraction, given the slight differences in loading levels between samples.

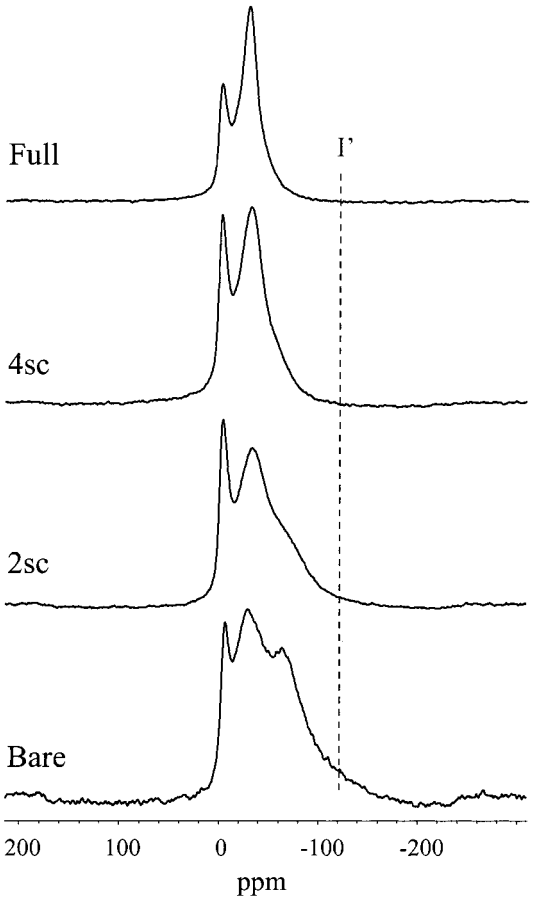

Figure 4. The ^{23}Na MAS NMR spectra of NaY, as a function of HFC-134 loading level, acquired at a spinning speed of 21 kHz. The dashed line indicates the position of one of the discontinuities from the resonance of the site I′ cations.

These results are consistent with our earlier proposal that HFC-134 binding results in a migration of the SI′ cations from the sodalite cages to positions in the supercages, where they can bind to the HFC molecules. The value of η for the new site

(35) Massiot, D.; Bessada, C.; Coutures, J. P.; Taulelle, F. *J. Magn. Reson.* **1990**, *90*, 231.

Table 2. ^{23}Na NMR Parameters for *x*HFC-134/NaY Obtained by 2D MQMAS NMR and by Simulating the ^{23}Na MAS NMR Spectrum[a]

	Ω/ppm (calcd value)	δ_{iso}/ppm	QCC/MHz	η	Na/uc this work	Na/uc X-ray[8]
2HFC-134/NaY						
SI	12.3 ± 1 (12.6)	1	1.2 ± 0.1	0.05 ± 0.05	8	3.8
new	35 ± 3 (35)	−5	2.8 ± 0.1	0.6 ± 0.1	14	22.7
SII	67 ± 5 (67)	−7	3.9 ± 0.15	0.05 ± 0.05	31	20.4
SII′						5
fully loaded HFC-134/NaY						
SI	16.2 ± 1 (16.4)	2	1.2 ± 0.1	0.05 ± 0.05	9	3.8[b]
new	−10 ± 3 (−11)	−13	2.2 ± 0.1	0.9 ± 0.1	27	27.8[b]
SII	26 ± 5 (25)	−8	3.0 ± 0.15	0.05 ± 0.05	16	21.4[b]
SII′						3[b]

[a] Calculated values for Ω are obtained from eq 1, with the values of the QCC and η used in the simulation of the Experimental Spectra; experimental values are extracted from the MQMAS data. Cation occupancies of the "new" site are compared with those obtained by X-ray diffraction (at 100 K) for the SIII′ position. [b] 4HFC-134/NaY.

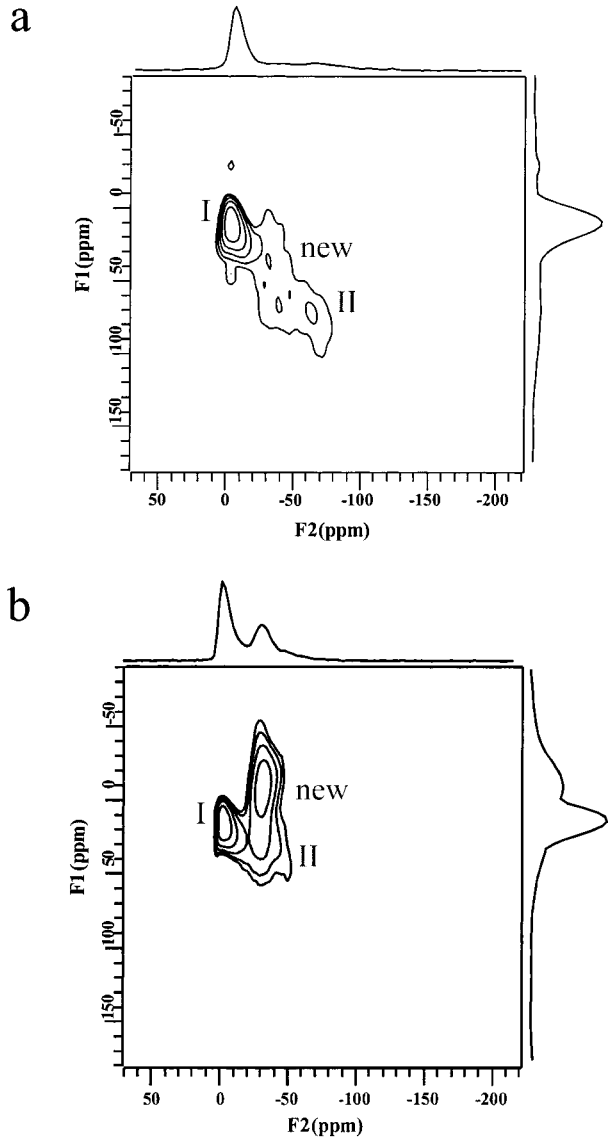

Figure 5. The 2D ^{23}Na triple quantum MAS NMR spectrum of (a) 2HFC-134/NaY and (b) fully loaded HFC-134/NaY after shearing, with the projections on the F1 and F2 dimensions. t_1 increments of 12.8 μs were used for both samples. 4800 FIDs were recorded for each t_1 increment for both samples; all other experimental details are similar to those described in Figure 3.

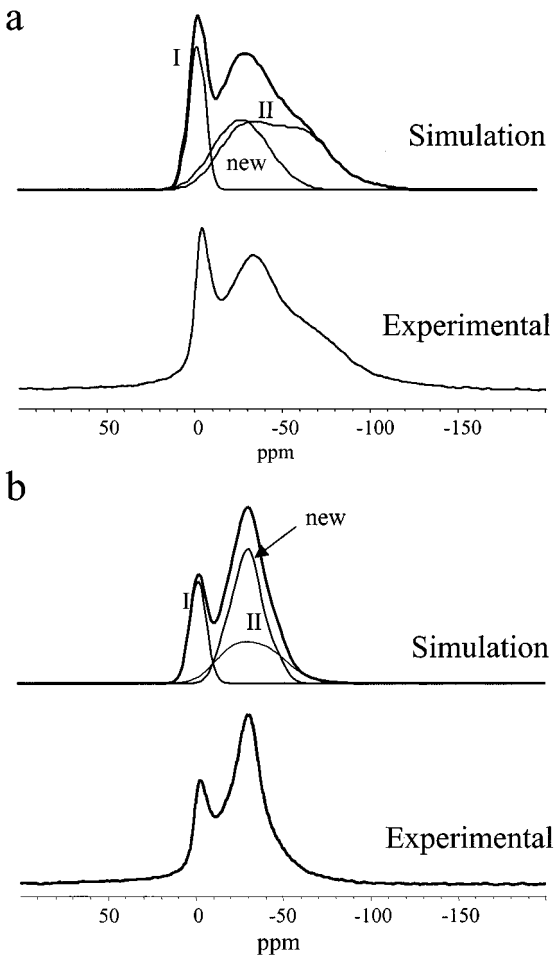

Figure 6. The simulated and experimental ^{23}Na MAS NMR spectra of (a) 2HFC-134/NaY and (b) fully loaded HFC-134/NaY.

does not appear to be consistent with the postulate by Bosch et al. that the changes in QCC and η are due to hydrogen bonding of the HFC to the zeolite framework, and associated charge redistributions: The SI′ cations are bound to the O(3) atoms [Na(I′)−O(3) = 2.3 Å],[8] which point directly into the sodalite cage. These O(3) atoms are not directly accessible to the HFC molecules, thus any changes in their partial charges must be inductive. The next-nearest anions are the O(2) oxygens that are 3 Å away. These anions are clearly affected by HFC binding, and this binding could be asymmetric. Thus, it is possible that the local symmetry at the SI′ will be reduced due to asymmetric binding arrangements of the HFC molecules. But it is nonetheless surprising that binding to the second anion coordination sphere is responsible for such a dramatic change in η from essentially zero to close to 1.

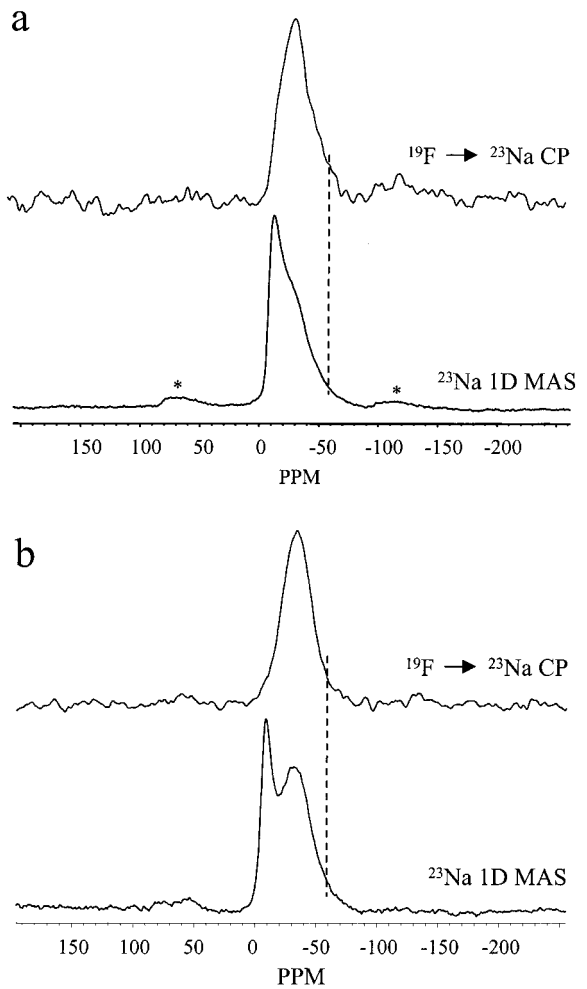

Figure 7. The ^{23}Na MAS and ^{19}F → ^{23}Na CP MAS spectra of (a) 2HFC-134a/NaY and (b) 4HFC-134a/NaY at −120 °C. A spinning speed of of 8 kHz and a contact time of 375 μsec were used for the CP experiments. A ^{19}F radio frequency field strength of 20 kHz and a ^{23}Na radio frequency field strength of 10 kHz were used and 1000−2000 FIDs were recorded for the CP spectra. The dashed line and asterisk mark the resonance from the site II cations and spinning sidebands, respectively.

To test the proposal by Bosch et al. in more detail, ^{19}F → ^{23}Na CP MAS NMR experiments were performed at −120 °C,a temperature at which the isotropic motions of the HFC gas molecules are essentially frozen out.[11] We were unable to use fast spinning speeds for the low-temperature experiments. However, the ^{23}Na MAS NMR spectra of both 2HFC-134/s.c and 4HFC-134/s.c. loading levels, at a slower spinning speed of 8 kHz, were similar to those obtained at a higher spinning speed of 18 kHz, at room temperature. Previous ^{23}Na VT MAS NMR experiments on HFC-134/NaY samples at different loading levels have shown that line shapes of the broad NMR resonances from the site II and III′/I′ cations become broader, as the temperature is decreased.[8] This broadening may be ascribed to either (i) stronger interactions between the HFC molecules and specific II and III′ cations as the HFC motion is frozen out or (ii) a more significant charge redistributions caused by a stronger hydrogen bonding at lower temperatures. Nonetheless, a spinning speed of 8 kHz was considered adequate for these CP studies, since the QCCs of the sodium cations are still sufficiently small at low temperatures on adsorption of HFC-134.

A broad resonance centered at ∼ −33 ppm and a shoulder at ∼ −50 ppm are observed at both loading levels, in the ^{19}F → ^{23}Na CP MAS NMR spectra shown in Figure 7. The site I cations are not detected, indicating that polarization is only transferred to cations in close proximity to the HFCs. Other than the absence of the resonance from the site I cations, the line shapes of the CP MAS spectra are very similar to those of the 1D MAS spectra. This suggests that both sets of sodium cations originally located in the site II and I′ positions are located nearby the HFC molecules, which supports the theory that the site I′ cations migrate into the supercages to interact with the HFC molecules.

HFC-134/NaX. Similar ^{23}Na MAS NMR experiments were performed on HFC-134/NaX systems to investigate changes in the occupancy of sodium cations in NaX on adsorption of HFC-134 (Figure 8). As the loading level is increased, the broad resonance from the site II cations narrows considerably due to a reduction of the QCC, as was observed for the HFC-134/NaY system. However, no significant changes in the frequency and line shape of resonance assigned to site I′ cations are observed, unlike in the HFC-134/NaY system. The NMR resonance from the site I cations (∼1 ppm) is split into two sharp resonances (2 and −5.3 ppm) and the resonance at −5.3 ppm grows in intensity as the loading level is increased.

The two sharp resonances from the site I cations appear at different positions in the F1 dimension of the ^{23}Na MQMAS NMR spectra of HFC-134/NaX (Figure 9), implying that the sodium cations originally in the site I position have different local environments on HFC-134 gas adsorption. The signal from the site II cations shifts to a lower frequency in the F1 dimension as the loading level is increased (see Figures 3b and 9), indicating that the QCC of the site II cations is again reduced at higher loading levels. For the site III cations, the two distinct signals from the sodium cations in sites III′(1,2) and III′(3) are no longer clearly discernible in the MQMAS NMR spectra of 2HFC-134/NaX (Figure 9a), the new SIII site appearing at a higher frequency in the F1 dimension than was observed in bare NaX. On the other hand, the two types of site III cations are again resolved for the fully loaded sample in Figure 9b. The site I′ cations are observed in a similar position (100 and −140 ppm in F1 and F2 dimension, respectively) for both bare NaX and HFC-loaded samples, indicating that the effect of the HFC adsorption on the QCC and local environment of the site I′ cations is insignificant: for the fully loaded sample, the signal from the site I′ cations is not clearly observed with the contour levels used in Figure 9, due to its small relative intensity caused by the very large QCC; the signal was, however, clearly visible in the MQMAS spectrum plotted with a lower contour level. This implies that the local environment of the site I′ cations is not significantly affected by the hydrogen bonding of HFC-134. Again this supports the conclusion that the significant changes in the QCC of the site I′ cations in *x*HFC-134/NaY systems arise from the migration of the sodium cations, and not from hydrogen-bonding interactions with the zeolite framework.

Experimental ^{23}Na MAS NMR spectra of 2HFC-134/NaX and fully loaded HFC-134/NaX were simulated with the NMR parameters obtained from the MQMAS NMR spectra (Figure 10). Good fits between the experimental and simulated spectra were obtained. The relative populations and the NMR parameters calculated from the simulations of the ^{23}Na MAS spectra are shown in Table 3. No significant changes in the relative populations were observed on adsorption of HFC-134 molecules, unlike for the HFC-134/NaY systems.

^{23}Na NMR of HFC-134a, -125, and -143/NaY. To determine whether cation migrations occur in the other hydrofluorocarbon systems, a systematic study with a series of hydrofluorocarbons

Table 3. ^{23}Na NMR Parameters for *x*HFC-134/NaX Samples Obtained by 2D MQMAS NMR and by Simulating the ^{23}Na MAS NMR Spectra[a]

	Ω/ppm (calcd value)	δ_{iso}/ppm	QCC/MHz	η	Na/uc
2HFC-134/NaX					
SI(1)	22 ± 1 (22)	3	1.3 ± 0.1	0.05 ± 0.05	1.5 ± 0.2
SI(2)	−7 ± 1 (−6)	−4.6	1.3 ± 0.1	0.05 ± 0.05	1.5 ± 0.2
SI′	104 ± 5 (103)	−20	5.4 ± 0.15	0.05 ± 0.05	28 ± 2
SII	100 ± 5 (100)	−8	4.6 ± 0.15	0.05 ± 0.05	32 ± 2
SIII′	17 ± 2 (18)	−12	3.0 ± 0.1	0.6 ± 0.1	22 ± 2
fully loaded HFC-134/NaX					
SI(1)	23 ± 1 (23)	3.4	1.3 ± 0.1	0.05 ± 0.05	1.3 ± 0.2
SI(2)	2 ± 1 (2)	−2.3	1.3 ± 0.1	0.05 ± 0.05	1.7 ± 0.2
SI′	96 ± 5 (96)	−20	5.3 ± 0.15	0.05 ± 0.05	28 ± 2
SII	65 ± 5 (65)	−5	3.7 ± 0.15	0.05 ± 0.05	32 ± 2
SIII′(1,2)	32 ± 2 (31)	−5	2.7 ± 0.1	0.6 ± 0.1	12 ± 1
SIII′(3)	−20 ± 2 (−20)	−14	2.0 ± 0.1	0.95 ± 0.05	10 ± 1

[a] Calculated values for Ω are obtained from eq 1.

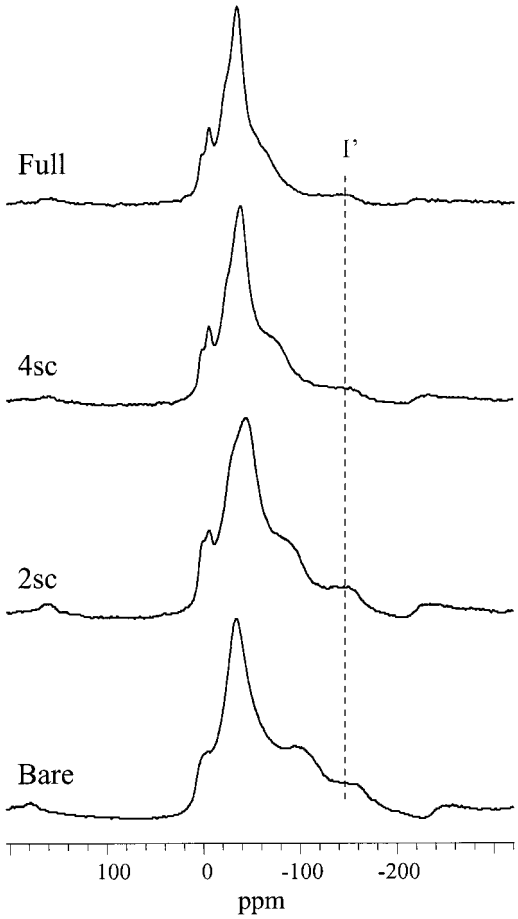

Figure 8. The ^{23}Na MAS NMR spectra of NaX, as a function of HFC-134 loading level, acquired at a spinning speed of 21 kHz. The dashed line marks the most obvious discontinuity in the resonance from the site I′ cations.

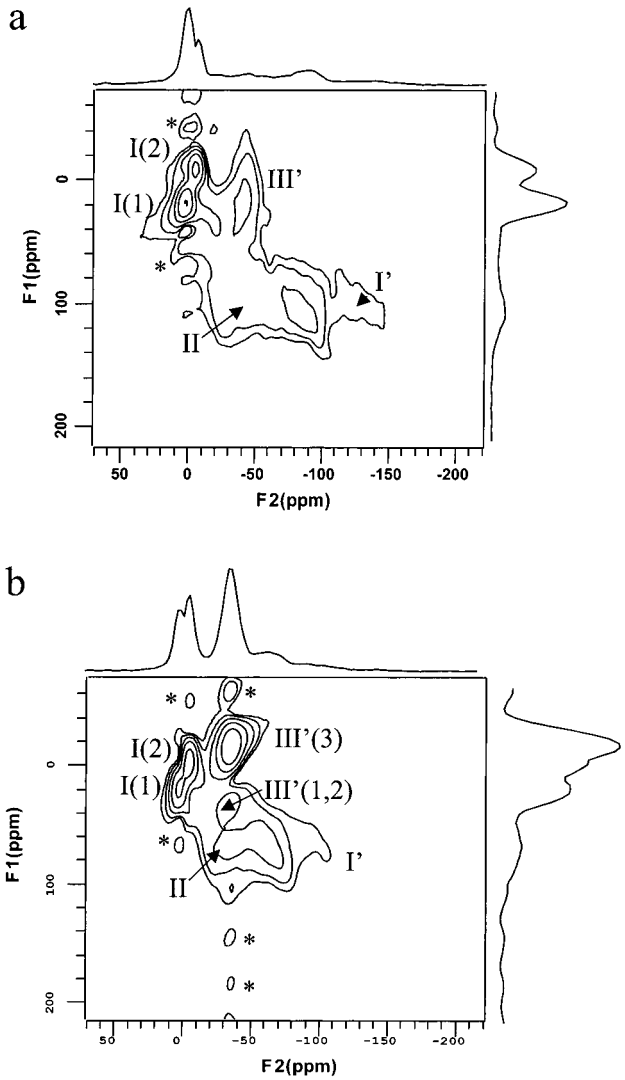

Figure 9. The 2D ^{23}Na triple quantum MAS NMR spectrum of (a) 2HFC-134/NaX and (b) fully loaded HFC-134/NaX, after shearing. t_1 increments of 9.3 μs were used for both samples, respectively. 6000 FIDs were recorded for each t_1 increment for both samples; all other experimental details are similar to those described in Figure 3. An asterisk denotes the artifacts originating from the insufficient t_1 data points used in the data collection.

was performed. Figure 11a shows a comparison of the ^{23}Na MAS line shapes of HFC-134, -134a, -143, and -125/NaY for a loading level of 4 molecules/s.c. HFC-134a, -143a, and -125 show similar behavior at this loading level. No evidence for a SI′ cation is observed, indicating that cation migration occurs in these systems too. The resonances of all the cations, other than the SIs, are broader and less intense than those observed for HFC-134/NaY. Part of this can be ascribed to the lower spinning speed. The broad resonance may be divided into a sharp component, which, based on previous assignments and simulations, is assigned to SIII′ cations, and a broader component, which is assigned to SII cations. The spectra obtained at a higher loading level show quite different behavior for HFC-134, -134a, and -125. A much broader resonance, with a more pronounced shoulder to higher frequency, is observed for HFC-125. This shoulder is ascribed to SII cations, which are less strongly coordinated to HFC molecules. Weaker binding of HFC-125 is

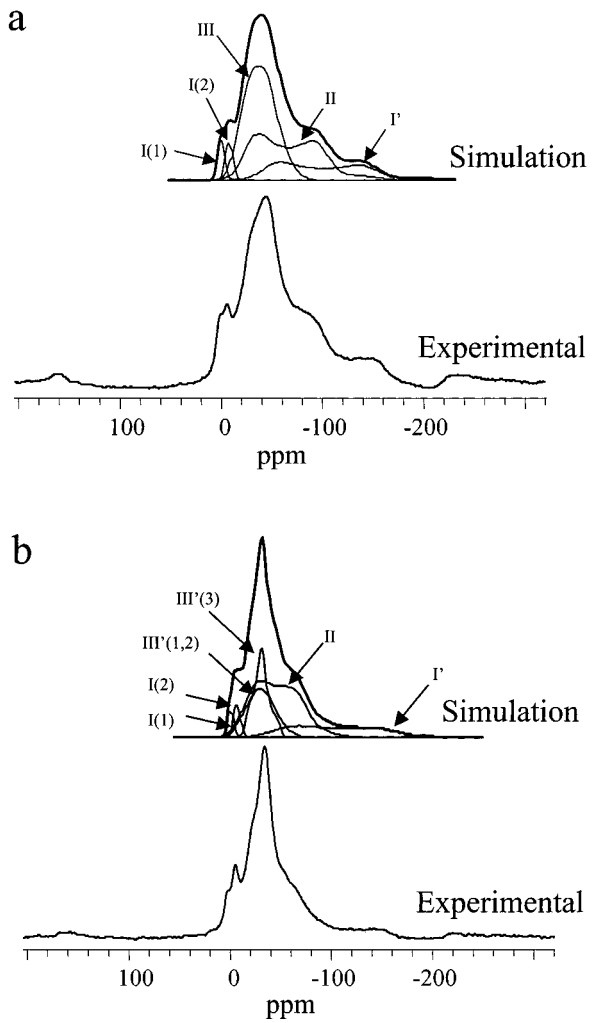

Figure 10. The simulated and experimental ^{23}Na MAS NMR spectra of (a) 2HFC-134/NaX and (b) fully loaded HFC-134/NaX.

consistent with the lower numbers of hydrogen atoms in this molecule, resulting in less H-bonding interactions with the framework, and a lower fluorine partial charge on the fluorine atoms, as proposed in our earlier CP study.[11]

^{23}Na VT NMR of Bare NaY. ^{23}Na VT MAS and MQMAS NMR experiments were performed on bare NaY above room temperature. Figure 12 shows the ^{23}Na VT MAS NMR spectra at a spinning speed of 10 kHz. As the temperature is increased, the resonance from the SI cations starts to broaden and at above 150 °C, additional intensity centered at around −30 ppm is observed. Similar behavior is also observed in the ^{23}Na VT MAS NMR spectra of a sample that was sealed in a quartz tube, indicating that the new resonance does not originate from the rehydration of the sample during the experiments. To investigate changes in the SI′ cations, ^{23}Na MAS NMR spectra were also obtained at a spinning speed of 21 kHz (Figure 13). As the temperature is increased, the broad resonance from the site I′ cations decreases in intensity, but is still observable even at 280 °C. Above 250 °C, the new resonance at approximately −30 ppm is also seen to shift to lower frequency.

MQMAS NMR experiments were performed on bare NaY at above room temperature, to try and resolve the new resonance. Signal-to-noise arguments resulted in the use of the larger volume probe, which was not capable of achieving very high radio frequency powers. Thus, the RIACT method was used for the MQMAS NMR experiments since resonances with large quadrupole coupling constants are, in theory, more readily

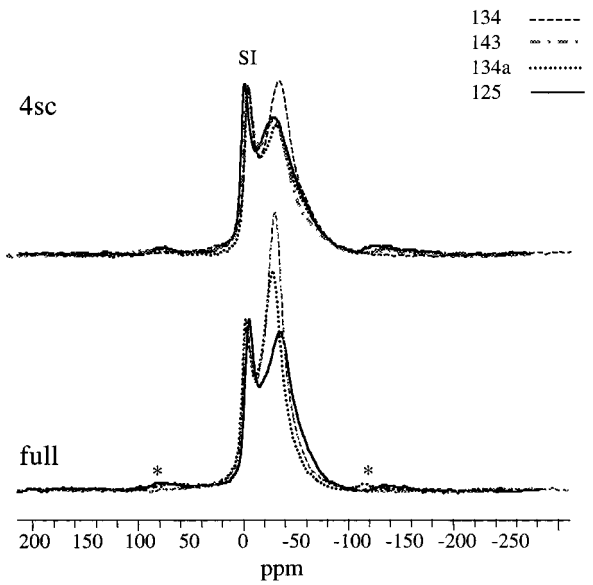

Figure 11. ^{23}Na MAS NMR spectra of HFC-134, -143a, -134a, and -125/NaY at loading levels of 4 molecules per supercage (a) and full loading (b); a spectrum of 143 at full loading was not available. The spectra have been normalized to the intensity of the resonance due to the SI cations. All spectra were acquired with spinning speeds of 10 kHz, apart from those of HFC-134, which were acquired at 21 kHz.

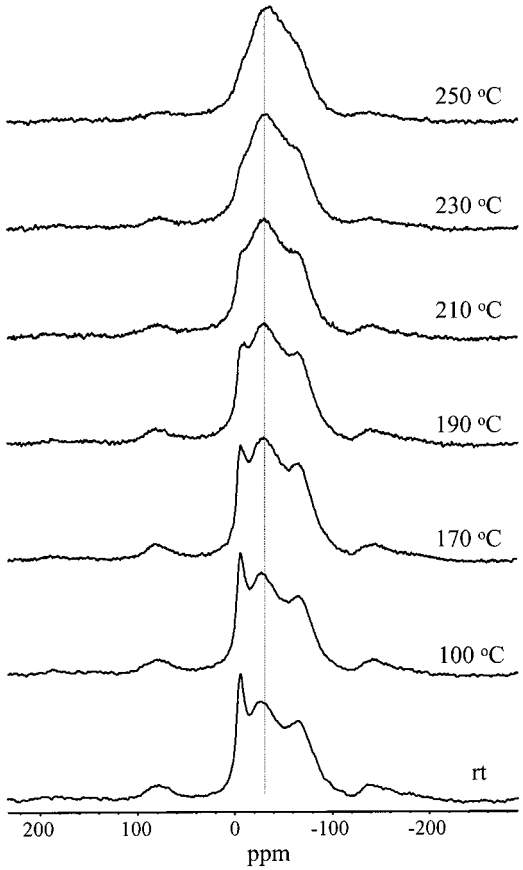

Figure 12. The ^{23}Na MAS NMR spectra of dehydrated bare NaY, as a function of temperature, acquired at a spinning speed of 10 kHz. The dashed line indicates the resonance from the new sodium cation resonance (∼ −30 ppm).

observable with this method.[30,36] Despite this, we were still unable to resolve the SI′ cations, presumably due to their large QCCs. However, the intensity of the signal from the site II

(36) Lim, K. H.; Grey, C. P. *Solid State NMR* **1998**, *13*, 101.

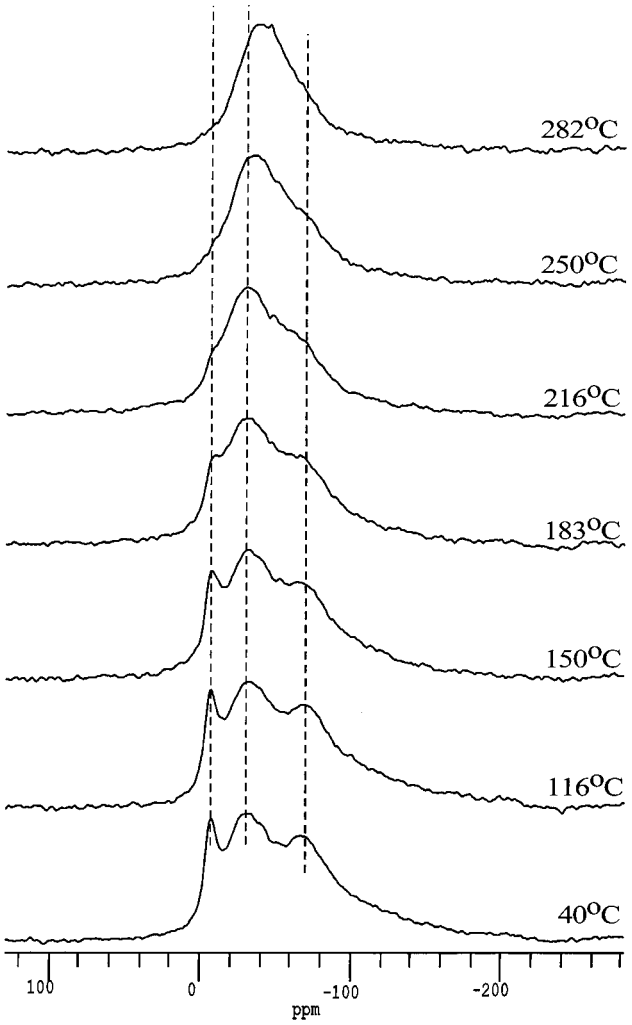

Figure 13. The ^{23}Na MAS NMR spectra of dehydrated bare NaY, as a function of temperature, acquired at a spinning speed of 21 kHz. The dashed lines indicate the resonances from the site I (~ -5 ppm), new sodium cations (~ -30 ppm), and low-frequency singularity of the resonance from the site II cations.

cations in the RIACT MQMAS NMR spectrum (Figure 14a) is much larger, in comparison to that in Figure 3b obtained with the *z*-filtered three-pulse MQMAS method (and the higher radio frequency power). Note that only the low-frequency singularity in the MAS line shape for the site II cations is observed in the RIACT spectra due to dependence of the excitation (and conversion) of the triple quantum coherences, on the orientation of the quadrupolar tensor with respect to the rotor axis, with this method.[36] As the temperature is increased, the resonance from the site I cations broadens in both the F1 and F2 dimensions and decreases in intensity relative to the site II resonance; no significant change in the line width and shift of the site II cation resonance is observed. A new resonance is clearly observed at above 150 °C in the VT RIACT MQMAS NMR spectra. At the highest temperature studied (250 °C), new intensity grows between the SII and new resonances, in the F2 dimension.

NMR parameters extracted from the MQMAS NMR spectra at 200 °C, and by simulation of the MAS spectra, indicate that the QCC and η of the SII cations remain unchanged from room temperature to 200 °C. An estimate of the QCC of the new site of $\sim$3 MHz ($\eta = 0.5$) was obtained from the RIACT spectra at 200 and 250 °C. Simulations of the experimental spectra are not expected to yield very accurate cation occupancies for the different sites, as the SI′ position was not observed in the MQMAS spectra. Nonetheless, simulations of the 10 kHz MAS spinning speed data at 200 °C showed that a drop of more than 75% for the occupancy of SI was observed.

The new resonance(s) observed at high temperature could, in theory, originate from a change in the local environment of the sodium cations or from fast chemical exchange between various sodium sites. Thus, a two-dimensional ^{23}Na magnetization exchange NMR experiment was performed on bare NaY at 250 °C, to investigate the chemical exchange between sodium cations. Figure 15 shows the 2D magnetization exchange NMR spectrum at 250 °C, along with four cross-sections through the 2D spectra. There is clearly significant off-diagonal intensity, indicating that magnetization exchange occurs. There are two sources of magnetization exchange: either spin-diffusion or chemical exchange. Given that a relatively short mixing time was used, combined with a relatively high spinning speed, it is likely that the major cause of the cross-peaks arises from chemical exchange between sites. To confirm this, the experiment was repeated at 150 °C, and no cross-peak intensity was observed, allowing us to rule out spin-diffusion as a significant cause of cross-peak formation at 250 °C.

The top slice of the spectrum acquired at 250 °C shows a slice through one of the singularities of the SII resonance, and clearly shows exchange with either the new resonance or the other major discontinuity of the SII resonance. The slice through the new resonance (and hence also the SII high-frequency discontinuity) shows much smaller off-diagonal intensity, the major cross-peak occurring with the SII resonance. One possible explanation for this phenomenum is that the new resonance arises from cations undergoing relatively fast exchange between different cation sites. The remaining SII cation positions are undergoing sufficient motion to result in cross-peaks (within a time frame of 5 ms), but are not exchanging positions sufficiently fast to result in a collapse of the 2nd-order quadrupolar line shape. The SI resonance is connected to some off-diagonal intensity, suggesting that these residual SI cations are not rigidly held in the lattice. The slight asymmetry of cross-peak intensities in the 2D spectrum is most likely due to T_1 noise in the F1 dimension, due to the relatively short T_1s (spin−lattice relaxation times) of the ^{23}Na resonances.

Discussion

Since both faujasite samples studied do not contain ordered Si/Al atoms, a disorder in the expected position of the cations, e.g., differences in the distance between the cations and framework oxygen atoms, or in the number of nearby aluminum atoms, is expected. This is likely to result in a distribution of the isotropic chemical shift and the quadrupolar interactions of the sodium cations, in each of the sites, accounting for the relatively broad singularities of the second-order quadrupolar powder patterns of the site II and I′ cations in the ^{23}Na MAS NMR spectra of bare NaX and NaY. The effect is expected to be three times larger in the triple quantum dimension (F1) of the MQMAS NMR spectra, accounting for the relatively poor resolution of the MQMAS spectra. The efficiency of the MQMAS method is strongly dependent on the QCC values: in general, the smaller the QCC, the stronger the intensity of the resonance in the MQMAS NMR spectrum for moderate QCC systems. This accounts for the enhancement of the SI resonance in the MQMAS spectra and makes it very difficult to identify a large QCC site, such as the SI′ site in the zeolites NaX and NaY, especially at moderate field strengths.[25,26] However, the site I′ cations in NaY, which have not been observed in previous

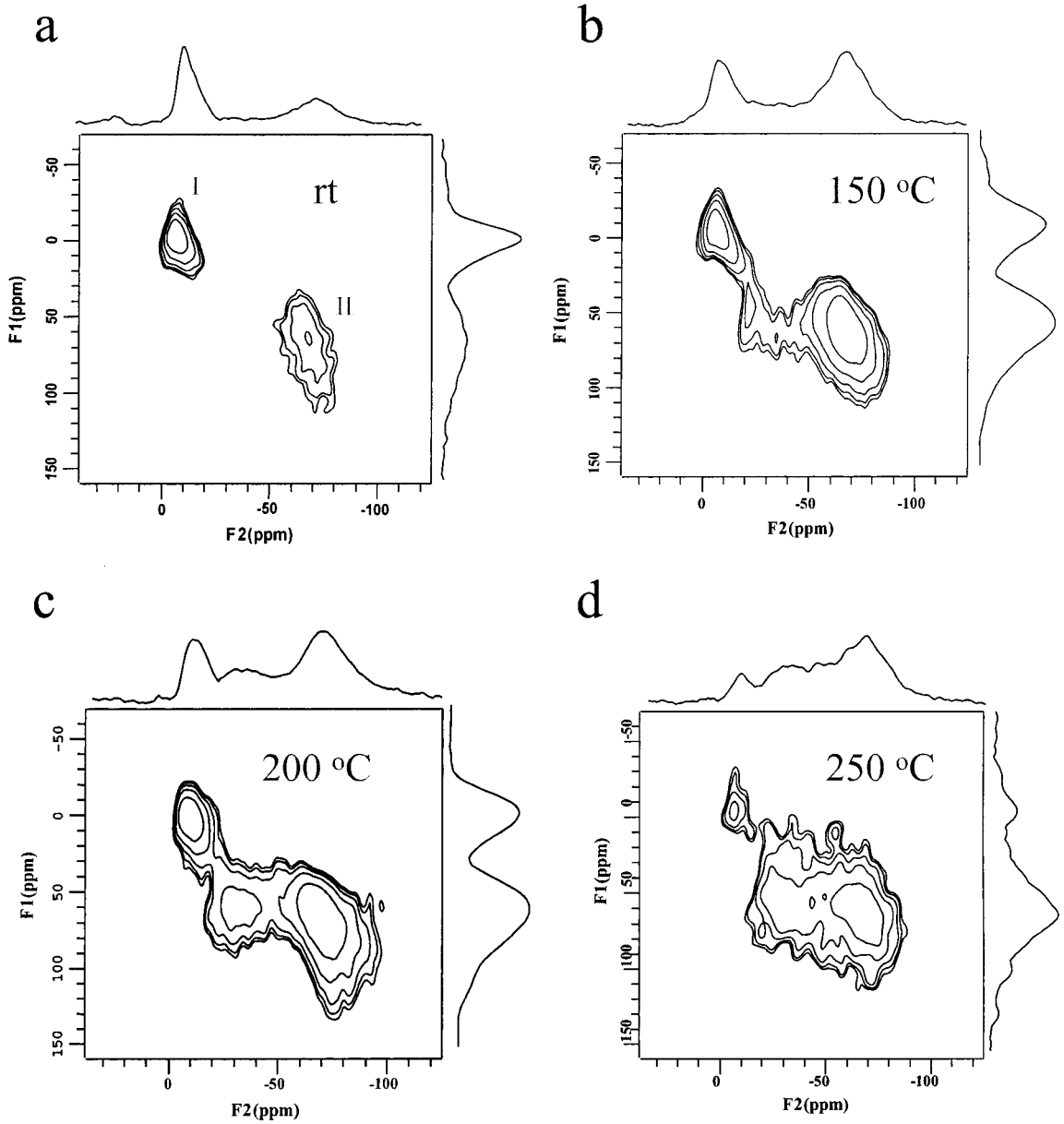

Figure 14. The 2D ^{23}Na RIACT triple quantum MAS NMR spectrum of dehydrated bare NaY at four temperatures, after shearing. A spinning speed of 10 kHz and t_1 increments of 25.6 μs were used. 480, 960, 1980, and 960 FIDs were recorded for each t_1 increment and 512 (t_2) × 58 (t_1), 512 (t_2) × 24 (t_1), 512 (t_2) × 26 (t_1), and 512 (t_2) × 36 (t_1) hypercomplex data points were acquired at room temperature (a), 150 (b), 200 (c) and 250 °C (d), respectively, and zero-filled to 512 (t_2) × 128 (t_1).

MQMAS studies,[25,26] could be detected in our MQMAS spectra when very fast MAS (21 kHz) and a high ^{23}Na radio frequency field strength (200 kHz) were used. The site I′ cations are more clearly observed in the MQMAS NMR spectrum of NaX since the occupancy of the site I′ cations is higher. No evidence was observed for the SI′ site in NaX with a smaller QCC, which has been ascribed to Na^+ coordinated to two aluminum atoms in the six ring.[17] On the basis of the previously reported NMR parameters, this resonance should be observed at 0 and ∼ −25 to −55 ppm in F1 and F2 dimensions of the MQMAS spectrum, respectively, and no intensity was observed in this region of the MQMAS NMR spectrum of our sample (Figure 3b).

Since two sodium cations occupy the site I position, per unit cell (Table 1), only 28 out of a total of 32 six-membered rings in the sodalite cages are available for occupancy by the SI′ cations, since the site I and I′ positions cannot be simultaneously occupied. The ^{23}Na MAS NMR spectrum of NaX may be well reproduced by assuming that all the available six-membered rings in the sodalite cages are fully occupied by sodium cations with a large QCC value (5.4 MHz), without considering the presence of any additional site I′ cations. Nonetheless, a significant increase in the QCC of the SI′ from NaY (4.9 MHz) to NaX (5.4) was observed, systems where the SI′ sites are primarily coordinated to six rings with two and three aluminum atoms, respectively, suggesting that the second type of SI′ site in NaX should also have a smaller QCC. Assuming the SI′ positions near 3Al atoms are preferentially occupied, there are likely to be no more than about 4 of these types of cations per unit cell. Thus, it is likely that a combination of the small numbers of the SI′ sites with two nearby Al atoms, the possible overlap with the SII cations (which show a distribution of QCCs/δ_{iso}'s themselves) and the large QCC SI′ cations, and the fact that the difference in the QCCs between the two SI′ local environments is not as large as predicted render it difficult to resolve the two separate SI′ local environments. Finally, one possible explanation for the better resolved sites in NaX, in

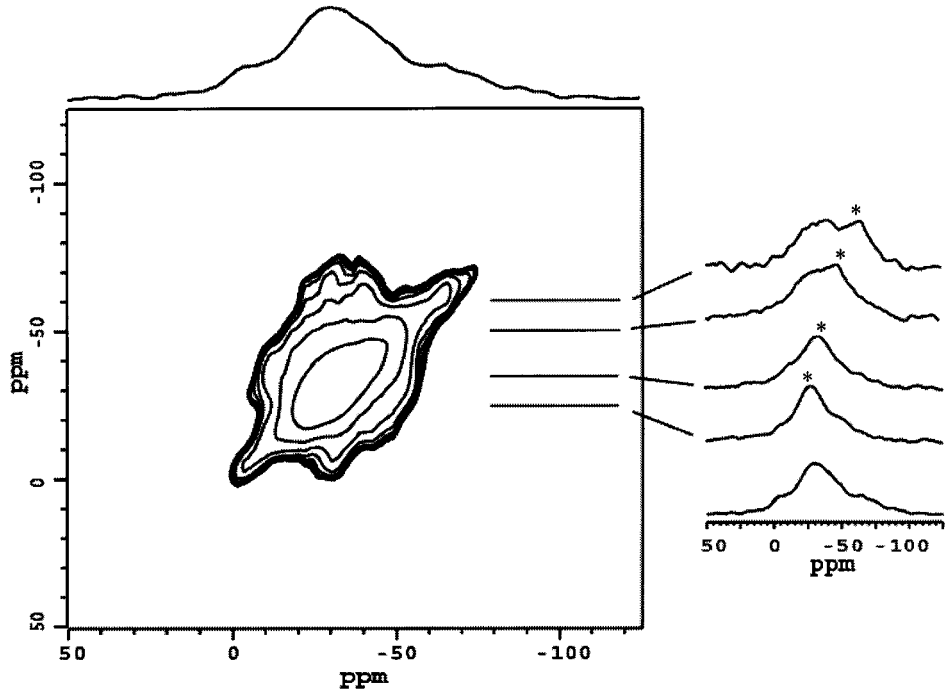

Figure 15. The 2D ^{23}Na magnetization exchange NMR spectrum of dehydrated bare NaY at 250 °C. A spinning speed of 20 kHz and t_1 increments of 15 μs were used. 3600 FIDs were recorded for each t_1 increment and 512 (t_2) × 44 (t_1) TPPI[39] data points were acquired and zero-filled to 512 (t_2) × 256 (t_1). A mixing time interval of 5 ms was used. Slices through the F2 dimension are plotted on the right-hand side of the figure, the asterisks on these spectra indicating the position of the diagonal in the 2D plot. The projection of the F2 dimension is shown above the 2D plot.

comparison to NaY, is that there are fewer different local environments for the SII and SI′ sites, since the Si/Al occupancies in NaX are closer to being strictly ordered, and thus a narrower distribution in QCCs/δ_{iso}s.

The combined ^{23}Na MAS and 2D MQMAS experiments showed that considerable changes in the occupancy of the extra-framework sodium cations in zeolite NaY occur on adsorption of HFC-134. Quantitative analysis of the ^{23}Na MAS spectra and the ^{19}F → ^{23}Na CP MAS NMR experiments on HFC-134/NaY systems provides convincing evidence that the site I′ cations in zeolite NaY migrate into the supercage where they can bind the HFC molecules, following gas adsorption. Even if we make different assignments of the SI′ and SII resonances to try and explain the changes on gas sorption, there can be no doubt that both resonances are affected by gas sorption. [For example, based on the discussion in the previous paragraph, one plausible alternative assignment of the two types of sites that is worth considering is that they arise from sodium cations with differing numbers or arrangements of Al atoms in the local coordination spheres; nonetheless, the SI′ cations must still be affected by the gas sorption.] The NMR parameters of the new sodium cation positions that result from the migration are similar to those of the site III′ cations in NaX, suggesting that the site III′ positions are occupied in HFC-134/NaY. The occupancies of the new sites are also close to those observed for the SIII positions in the XRD structural refinements, again consistent with the proposal. However, two different site III′ cations were not resolved in the MQMAS NMR spectrum of HFC-134/NaY, although a distribution in parameters was observed, presumably due to a variety of different modes of HFC gas binding. Furthermore, since the NMR parameters of bare SIII′ cations are similar to those of the new resonances, it suggests that the HFC molecules must be mobile at room temperatures, and not tightly bound to the cation positions. The decrease in the relative populations of the site II cations is also observed with increased gas loading level, in HFC-134/NaY system. This is consistent with our previous X-ray diffraction study, which proposed that the binding of the HFC molecules to the site III′ cations becomes more energetically favorable than binding to the site II cations at high loading levels, since site III′ cations can interact simultaneously with more than one HFC molecule.[8] The ^{23}Na NMR spectra of the other HFC/NaY samples show that the cation migrations are not limited to the HFC-134 system, but occur for all the HFC systems studied.

No significant changes in the occupancies of the sodium cations were observed for the HFC-134/NaX systems. Interestingly, the two site III′ cations resolved in bare NaX are not resolved at low loading levels, but are at high loading levels, suggesting that even in the NaX systems, small changes of cation positions occur within the supercages, as a function of the loading levels, as the positions of the site III′ cations readjust to maximize the HFC−Na interactions. The site I cations are affected by gas loading, in both the NaX and NaY systems, but in a different manner. For HFC-134/NaY, the SI population increases with increased gas loading level. This provides further support for the decrease in SI′ population, since the SI population in the bare material is limited by the SI′ population, since both sites cannot be simultaneously populated. In the HFC-134/NaX system, the total SI population remains unchanged (again consistent with the lack of change in SI′ population), but the SI resonance splits into two, the resonance at lower frequency (∼ −5.3 ppm) increasing in intensity as the loading level is increased. Neither of the two sharp SI resonances were observed in the ^{19}F → ^{23}Na CP MAS NMR spectra of the HFC-134/NaX systems, indicating that both these resonances originate from cations that are not bound to HFC molecules,[10] but must result from SI cations with slightly different local environments on adsorption of HFC-134. Thus it is clear that changes in the supercages, which result in changes in T−O−T angles, rearrangements of local cation arrangements, or the charge redistribution caused by the hydrogen-bonding interactions between the HFC molecules and the zeolite framework, do perturb the

SI cations slightly. The SI resonance, since it is associated with a much smaller QCC, is extremely sensitive to these small changes. Note that much smaller shifts in δ_{iso} are observed for SI in NaY, on gas loading. Further studies using different gas molecules (benzene and $CHCl_3$) are currently being performed to understand this behavior more fully.

The lack of changes in SI′ populations are consistent with our model for HFC-134 binding in these systems, obtained from XRD studies. The HFC molecule was proposed to bind at both ends to two separate cations, in an arrangement that maximizes cation and H-bonding interactions. The NaX system already contains ample cations in the supercages and is already optimized for HFC binding. These proposals are consistent with heats of sorption for these systems, where a much larger exothermic process is observed for NaX ($\Delta H_{abs} \approx -76$ kJ mol^{-1}, at low coverages, from calorimetry measurement), in comparison to that for NaY, estimated from the adsorption isotherm data ($\approx$56 kJ mol^{-1}).[37] The lower heat for NaY is ascribed to both a decrease in H-bonding interactions and the energy cost associated with cation migration.

Cation motion was observed in the bare, dehydrated systems, at temperatures quite close to room temperature (>150 °C), suggesting that cation positions are not rigidly fixed, and are extremely likely to be responsive to gas sorption. The combination of the ^{23}Na MAS and MQMAS NMR experiments showed that the resonance from the site I cations starts to broaden and a new resonance at ~ -30 ppm is observed above 150 °C. The relative intensity of the resonance from the site I′ cations also decreases as the temperature increases. As mentioned in the Introduction, there are two possible site I positions, within the hexagonal prism (see Figure 1), located on either side of the mirror plane which divides the two six-rings. A plausible suggestion for the disappearance of the SI resonances is that at high temperatures the SI cations can jump from one SI position to another, and also into the SI′ positions that are located on either side of the double six-rings, resulting in a resonance with a QCC intermediate between that of the SI and SI′ positions; the QCC of 3 MHz (estimated from the RIACT spectrum) is consistent with this suggestion. Since the SI cations are nominally six-coordinated, they may be expected to be the least mobile of all the cations. However, there are at least two explanations for this. First, since the SI resonances are much narrower than the resonances of the other cations, the spectra are much more sensitive to any mobility of these cations. Second, our earlier discussion of cation distributions for NaX, and the different local environments for SI′, strongly suggests that the SI′ cations occupy six-rings with higher numbers of aluminum atoms, leaving the SI to occupy local environments near six rings with a reduced number of aluminum atoms. These SI ions are then expected to be less tightly coordinated to the framework. The change in the population of the site I cation is not, however, large enough to account for all the intensity of the new resonance. Thus, at least some of the site I′ cations must also be involved in the jump processes. Very similar behavior was observed in the variable-temperature spectra of the HFC-134a/NaY samples, but the motion of the SI cations commenced at a lower temperature than for bare NaY.[38] In this case, the increased mobility may be due to the removal of other SI′ ions in the sodalite cages, reducing the cation electrostatic repulsions in the cages (or reducing the O(3)−O(3) distances slightly). The 2D magnetization exchange shows that some of the SII cations are mobile at 250 °C, and the shift of the new resonance at temperatures above 250 °C is then ascribed to mobility involving all the different sites. Finally, some of the changes in the spectra are also likely to be caused by small changes in occupancies of the different sites as a function of temperature. Entropic reasons alone would suggest that SIII positions become preferred over SII positions, and SI′ over SI (if the split position model is not taken into account), at higher temperatures, simply due to the larger numbers of these sites. An increase in SIII occupancy by Cs^+ was observed in Cs(Na)Y at higher temperatures, consistent with this suggestion.[7] Clearly, more extensive studies using different types of zeolites are still required to understand the changes and causes of the distribution of the extra-framework cations at high temperatures. These studies, however, clearly indicate that cation migrations through six-ring windows, which we believe occur in the HFC/NaY systems, are feasible at moderate temperatures, and must be associated with activation energies that are not energetically prohibitive, even at room temperature.

Conclusions

We demonstrated that large QCC sites in dehydrated zeolites NaX and Y can be characterized by using MQMAS, combined with very fast MAS (21 kHz) and high radio frequency field strengths (200 kHz). Four sodium sites (I, II, I′) including hydrated sodium cations and five sites (I, III′(1,2), III′(3), II, I′) were identified in dehydrated bare NaY and NaX, respectively. Quantitative analysis of the ^{23}Na MAS spectrum showed that a considerable rearrangement of the extra-framework cations in NaY, including migration of the site I′ cations to the supercage, occurred on adsorption of HFC-134 molecules. On the other hand, the populations of the sodium cations remain unchanged on adsorption of HFC-134 molecules onto zeolite NaX. ^{23}Na MAS NMR spectra of HFC-134a, -125, and -143a indicate that cation migrations occur in these systems too, and the phenomenum is not limited to HFC-134. It is clear that although hydrogen bonding of the HFCs to the zeolite framework does induce some spectra changes that are observable in the ^{23}Na MAS NMR spectra, e.g., HFC-134 adsorption results in two different SI resonances in NaX, the effects are not sufficient to account for all the spectral changes. Of particular note, no change in the QCC of the SI′ resonance is observed in NaX on gas sorption, a system where H-bonding is expected to be significant.

Variable-temperature NMR studies of dehydrated bare NaY show that cations in these systems are not rigidly held in their different sites. Cation jump processes, involving jumps through six-ring windows, were proposed to occur above 150 °C. This result has important implications because it indicates that if these processes can occur at moderate temperatures in the bare systems, then cation jumps (and longer range migrations), following gas sorption, cannot be ruled out on the basis of kinetic arguments.

Finally, we have shown that the combination of MQMAS method and simulation of the MAS NMR spectrum provides an effective method for extracting NMR parameters, and more importantly, relative site populations in these gas-loaded zeolites. This approach should prove useful in the analysis of cation populations following sorption of a whole variety of gases.

Acknowledgment. Funding from the Basic Energy Sciences Program at the Department of Energy (DE-FG02-96ER14681) is gratefully acknowledged. We thank Michael Ciraolo for his help with aspects of this work.

JA001281D

(37) Savitz, S. S.; Siperstein, F. R.; Huber, R.; Tieri, S. M.; Gorte, R. J.; Myers, A. L.; Grey, C. P.; Corbin, D. R. *J. Phys. Chem. B* **1999**, *103*, 8283.

(38) Grey, C. P.; Ciraolo, M. F.; Lim, K. H. *Proc. 12th Internat. Zeolite Conf.* **1998**, 2301.